Photothermoelastic interactions under Moore-Gibson-Thompson thermoelasticity

Rajneesh Kumar[1], Nidhi Sharma[2] and Supriya Chopra[*3]

[1]Department of Mathematics, Kurukshetra University, Kurukshetra, Haryana, India
[2]Department of Mathematics, Maharishi Markandeshwar University, Mullana, Ambala, Haryana, India
[3]Department of Mathematics, Government College for Women, Ambala city, Haryana, India

Abstract. In the present work, a new photothermoelastic model based on Moore-Gibson-Thompson theory has been constructed. The governing equations for orthotropic photothermoelastic plate are simplified for two-dimension model. Laplace and Fourier transforms are employed after converting the system of equations into dimensionless form. The problem is examined due to various specified sources. Moving normal force, ramp type thermal source and carrier density periodic loading are taken to explore the application of the assumed model. Various field quantities like displacements, stresses, temperature distribution and carrier density distribution are obtained in the transformed domain. The problem is validated by numerical computation for a given material and numerical obtained results are depicted in form of graphs to show the impact of various theories of thermoelasticity along with impact of moving velocity, ramp type and periodic loading parameters. Some special cases are also explored. The results obtained in this paper can be used to design various semiconductor elements during the coupled thermal, plasma and elastic wave and other fields in the material science, physical engineering.

1. Introduction

Analysis of mechanical and thermal interaction within a solid medium is of emended significance in various scientific fields. There are few examples such as high energy particle accelerated devices, modern aeronautical and astronomical engineering and different system exploited in nuclear and industrial applications with the consideration of second sound effect in thermoelastic model plays a significant role in analysing elastic body with in a variety of scientific and technological fields. In contradiction with physical observation the infinite thermal propagation speed is observed through conventional uncoupled theories.

The coupled thermoelasticity proposed by Biot (1956) in order to eradicate the classic uncoupled principle's inherent paradox. This paradox suggests that elastic changes have no temperature influence. The heat equations for both diffusion theories indicate that the heat wave

---

∗Corresponding author, Assistant Professor, E-mail: chopra.s22@gmail.com

propagation rates are unlike physical observations. Generalized thermoelasticity theories are designed to solve the weaknesses and shortcomings inherent in classic dynamic thermoelasticity coupled theory, which enables the thermal signal to propagate with unlimited speed.

The generalized thermoelasticity theory takes the effect of the coupling between strain rate and temperature into account, but the resulting coupling equations are hyperbolic. Thus, the inconsistency in the classic combined theory is removed with regard to the infinite speed of heat propagation. One of the generalized theories of thermoelasticity updated, which included the implementation of a new law of thermal conductivity to replace the Fourier conventional law was proposed by Lord and Shulman (1967). This amended legislation involves heat flow and its time-related partial derivative.

Green and Naghdi (1991, 1992, 1993) derived three models in thermoelasticity which are labelled as GN-I, II and III models. The linearized form of model-I reduces to classical heat conduction theory whereas linearized version of model-II and III permit propagation of thermal waves at finite speed.GN-II (1993) shows a feature which makes it different from other thermoelastic models as it does not allow dissipation of thermal energy. The model GN-III (1992) contains the thermal displacement gradient alongwith temperature gradient among the constitutive variables and admits the dissipation of energy.

Tzou (1995) proposed the dual-phase heat conduction law which is a more common one with two different phase delays, one in the heat flow vector and the second in the temperature gradient, which takes into account the effects of the microstructure on the heat transmission mechanism, in order to evaluate the delayed reaction caused by the microstructure effects over time. One of the most recent advances in the theory of thermoelasticity is the three-phase lags suggested by Roychoudhari (2007). This model also has phase delays of thermal displacement gradients, in addition to the phase lags in the hot flux vector and temperature gradient. These two suggestions, involving different derivatives as the Taylor spectrum approaches the heat flow and temperature gradients, assume that the suggestion by Roychoudhari seeks to restore Green and Naghdi models if various Taylor approaches are taken into account.

Othman *et al*. (2009) examine the transient wave caused by a line heat source with a uniform velocity inside isotropic homogeneous thermoelastic perfectly conducting half-space permeated into a uniform magnetic field. Sharma (2010) investigated the boundary value problems in generalized thermodiffusive elastic medium. Abbas (2011) employed the theory of thermoelasticity with energy dissipation to study plane waves in a fiber-reinforced anisotropic thermoelastic half-space. Sharma *et al*. (2012) studied the propagation of Lamb waves in a homogeneous isotropic thermoelastic micropolar solid with two temperature bordered with layers or half-spaces of inviscid liquid.

Abbas (2014a) obtained thermoelastic damping and frequency shift of a thermoelastic hollow sphere in the context of generalized thermoelasticity theory. Abbas (2014b) considered the infinite fiberreinforced anisotropic plate with time fractional ordered derivative by using Green and Naghdi type II theory of thermoelasticity. Abo-Dahab and Lotfy (2015) investigated a thermal shock problem in a fiber reinforce fractional ordered thermoelastic half space with rotation and uniform magnetic field. Marin *et al*. (2015) presented the domain of influence theorem in anisotropic generalized thermoelastic material. Abbas (2015) examine a problem of spherical cavity due to ramp type heating in a fractional order thermoelastic diffusion infinite medium by employing eigen value approach. Hobiny and Abbas (2018) obtained an analytic solution for the hyperbolic bio heat model under a new heat source.

Semiconducting materials have been widely applied in modern engineering applications with

the present development of technologies. When a semiconductor surface is exposed to a beam of laser, some electrons will be excited. In this case, the photo-excited free carriers will be produced with non-radiative transitions, and a recombination between electron and hole plasma occurs. Many efforts are made to explore the nature of semiconductors in last few years and the technique adopted is photo acoustic and photo thermal technology.

Photoacoustic (PA) and photothermal (PT) science and technology have extensively developed new methods in the investigation of semiconductors and microelectronic structures during the last few years. PA and PT techniques were recently established as diagnostic methods with good sensitivity to the dynamics of photoexcited carrier (Mandelis 1987, Almond and Patel 1996, Mandelis and Michaelian 1997, Nikolic and Todorovic 1989). Photogeneration of electron-hole pairs, i.e., the carriers-diffusion wave or plasma wave, generated by an absorbed intensity modulated laser beam, may, play a dominant role in PA and PT experiments for most semiconductor materials. Depth dependent plasma waves contribute to the generation of periodic heat and mechanical vibrations, i.e., thermal and elastic waves. This mechanism of elastic wave generation is a specific of semi-conductors. The electronic deformation mechanism is based on the fact that photogenerated plasma in the semiconductor causes deformation of the crystal lattice, i.e., deformation of the potential of the conduction and valence bands in the semiconductor. Thus, photoexcited carries may cause local strain in the sample. This strain in turn may produce plasma waves in the semiconductor in a manner analogous to thermal wave generation by local periodic elastic deformation.

Many problems of deformation and wave propagation are investigated by different authors due to its academic importance and physical application. Lotfy and Othman (2011) examine the effect of variable thermal conductivity during the photo thermal diffusion problem of semiconductor medium due to mechanical and thermal source. Lofty (2019) describe the effect of variable thermal conductivity during a photothermal-diffusion process. Lotfy *et al*. (2020) expressed the novel mathematical model under the effect of Thomson heating of a semi-infinite semiconductor elastic medium in the presence of magnetic field subjected to a laser pulse. Khasim *et al*. (2020) investigated wave propagation in a photohermoelastic half space with refined multi dual phase lag due to mechanical and thermal loading. Mahdy *et al*. (2020) investigated electromagnetic hall current and fractional heat order for micro- temperature in photothermoelastic half space subjected to thermomechanical loading.

Jahangir *et al*. (2020) discussed the reflection of thermoelastic waves in semiconducting medium. Zenkour (2020) constructed the generalized photothermoelastic problem of beam with modified multi-phase-lag photothermoelasticity theory. Hobiny *et al*. (2021) investigated two-dimensional photothermoelastic problem in semi-conductor material influenced by ramp-type heating. Zakaria *et al*. (2021) constructed a modified generalized fractional photothermeolastic model on the basis of the fractional calculus technique. Sharma and Kumar (2021) developed a dynamic mathematical model of photothermoelastic (semiconductor) medium to analyze the deformation due to inclined loads. Sharma and Kumar (2022) examined photothermoelastic deformation in dual phase lag model due to concentrated inclined load. Kumar *et al*. (2022) investigated deformation due to thermomechanical carrier density loading in orthotropic photothermoelastic plate. Mohamed *et al*. (2022) constructed a model to understand the photothermal excitation process of optical thermal transfer and the interaction between elastic, plasma, thermal waves during a microstretch case. Saeed *et al*. (2022) examined the impact of the magnetic field on the non-homogeneous elastic semiconductor material.

The Moore-Gibson-Thompson equation has received immense level of interest in recent years.

Thompson (1972) developed this theory starting from a third-order differential equation, built in the context of some considerations related to fluid mechanics. Quintanilla (2019) proposed the modified heat equation after adding the relaxation parameter in the Green-Naghdi model of type-III. Conti (2020a, 2020b) examine some problems in Moore-Gibson-Thompson thermoelastic model. Quintanilla (2020) presented Moore-Gibson-Thompson thermoelastic model with two temperature.

Bazarra (2020) examined some problem on Moore-Gibson-Thompson thermoelastic model. Marin (2020) presented mixed initial-boundary value problem in the context of the Moore-Gibson-Thompson theory of thermoelasticity for dipolar bodies. Abouelregal *et al.* (2020) investigate the wave propagation in an isotropic and infinite body subjected to a continuous thermal line source based on Moore-Gibson-Thompson thermoelasticity theory. Abouelregal *et al.* (2021) obtained the solution of Moore-Gibson-Thompson equation for an unbounded medium with a cylindrical hole. Singh and Mukhopadhyay (2021) presented a Galerkin-type solution under the Moore-Gibson-Thompson thermoelasticity theory. Abouelregal *et al.* (2021) presented modified Moore-Gibson-Thompson photo-thermoelastic model for a rotating semiconductor half-space under magnetic field**.** Jangid *et al.* (2021) discussed the propagation of harmonic plane waves under the Moore-Gibson-Thompson thermoelasticity theory. Kumar and Mukhopadhyay (2020) discussed the thermoelastic damping in microbeam resonators based on Moore-Gibson-Thompson thermoelastic model.

The problem of solid mechanics should not be restricted to the isotropic numerically. Increasing use of anisotropic media demands that the study of photothermoelastic problems should be extended to anisotropic medium also. Due to many applications of MGT of semiconductor elastic media in modern physics through photo elastic thermal excitation process are used in many industrial applications leads to investigate deformation in photothermoelastic due to various sources under MGT. In this paper, deformation due to thermomechanical and carrier density loading in orthotropic photothermoelastic plate under Moore-Gibson-Thompson thermoelastic model has been studied. Laplace and Fourier transform are employed to solve the problem. The analytical expressions of normal stress, temperature distribution and carrier density distribution are computed in the transformed domain. However, the resulting quantities are obtained in the physical domain by using numerical inversion technique. The variations of stress component, temperature distribution and carrier density distribution are depicted graphically to demonstrate the effect of Moore-Gibson-Thomson thermoelastic model (2019), Classical thermoelastic model (1983), Lord and Shulman's model (1967) with one relaxation time, Green and Naghdi type-II model (1993) and Green and Naghdi type-III model (1992) along with different sources.

2. Elementary equations

The constitutive relation and the field equations for photothermoelastic based on Moore-Gibson-Thompson thermoelastic model in absence of body forces, heat sources and carrier photogeneration sources are described by Todorovic (2003, 2005), Pellicer and Quintanilla (2020)

$$t_{ij} = C_{ijkl}e_{kl} - \alpha_{ij}T - \gamma_{ij}N, \tag{1}$$

$$C_{ijkl}e_{kl,} - \alpha_{ij}T_{,h} - \gamma_{ij}N_{,h} = \rho\ddot{u}_l \tag{2}$$

$$K_{ij}\dot{T}_{,ij} + K^*_{ij}T_{,ij} = \left(1 + \tau_o \frac{\partial}{\partial t}\right)\left[\left(\rho C_e \ddot{T} + T_o \alpha_{ij}\dot{e}_{ij}\right) - \frac{E_g}{\tau}\frac{\partial N}{\partial t}\right] \tag{3}$$

$$D^*_{ij}N_{,ij} = \frac{\partial N}{\partial t} + \frac{N}{\tau} - \zeta \frac{T}{\tau} \quad (i, j, k, l, h=1, 2, 3) \tag{4}$$

where

τ_o the thermal relaxation time, C_{ijkl} elastic parameters, α_{ij} are coefficient of linear thermal expansion, γ_{ij} coefficient of electronic deformation, u_i components of displacement, T-the temperature distribution, T_o the reference temperature, $N = n - n_o$, n_o equilibrium carrier concentration, E_g the semiconductor energy gap, ρ-the medium density, t_{ij} the components of stress tensor, K_{ij} thermal conductivity, K^*_{ij} thermal conductivity rate, C_e the specific heat, $\zeta = \frac{\partial n_o}{\partial T}$ the thermal activation coupling parameter, τ-the photogenerated carrier lifetime, t-the time variable, D^*_{ij} the coefficients of carrier diffusion, e_{kl} the components of elastic strain.

The following cases arise:

Photothermoelasticity under Moore-Gibson-Thompson model in which K_1, K_3, K^*_1, K^*_3 and τ_o all are positive is limited to the following cases as:

(i) Classical thermoelastic (CTE) model is possible when
$$\tau_o = K^*_1 = K^*_3 = 0$$

(ii) Lord and Shulman's (LS) model can be attained as a limited case when
$$K^*_1 = K^*_3 = 0.$$

(iii)The introduced model makes it possible to obtain Green and Naghdi of type-II (GN-II) model when
$$\tau_o = K_1 = K_3 = 0.$$

(iv) Green and Naghdi type- III (GN-III) model can be obtained when
$$\tau_o = 0.$$

3. Formulation of the problem

An infinite orthotropic photothermoelastic plate under Moore-Gibson-Thompson (MGTE) model is considered. A plate having finite thickness $2d$ is homogeneous, isotropic and thermal conducting with initial uniform temperature T_o. The middle plane of the plate coincide with $x_1 - x_2$ plane such that $-d \leq x_3 \leq d$ and $-\infty < x_1, x_2 < \infty$, the origin of the coordinate system is taken at any point of the middle plane. The boundary surface $x_3 = \pm d$ is subjected to thermomechanical and carrier density loading. Let the $x_1 - x_3$ plane be taken as the plane of incidence and restrict our analysis to this plane, so that the physical field variables are function of x_1, x_2, t. Thus, the displacement components, temperature distribution and carrier density distribution are given by

$$u = \left(u_1(x_1, x_3, t), 0, u_3(x_1, x_3, t)\right), T = T(x_1, x_3, t) \text{ and } N = N(x_1, x_3, t), \tag{5}$$

We have used appropriate plane of symmetry, following Slaughter (2002) on the set of Eqs. (1)-(4) to derive the equations for orthotropic photothermoelastic solid for two dimensional problem with the aid of Eq. (5), take the following form

$$C_{11}\frac{\partial^2 u_1}{\partial x_1^2} + C_{55}\frac{\partial^2 u_1}{\partial x_3^2} + (C_{13}+C_{55})\frac{\partial^2 u_3}{\partial x_1 \partial x_3} - \alpha_1\frac{\partial T}{\partial x_1} - \gamma_1\frac{\partial N}{\partial x_1} = \rho\frac{\partial^2 u_1}{\partial t^2} \tag{6}$$

$$C_{55}\frac{\partial^2 u_3}{\partial x_1^2} + C_{33}\frac{\partial^2 u_3}{\partial x_3^2} + (C_{13}+C_{55})\frac{\partial^2 u_1}{\partial x_1 \partial x_3} - \alpha_3\frac{\partial T}{\partial x_3} - \gamma_3\frac{\partial N}{\partial x_3} = \rho\frac{\partial^2 u_3}{\partial t^2}, \tag{7}$$

$$K_1\frac{\partial^3 T}{\partial x_1^2 \partial t} + K_3\frac{\partial^3 T}{\partial x_3^2 \partial t} + K_1^*\frac{\partial^2 T}{\partial x_1^2} + K_3^*\frac{\partial^2 T}{\partial x_3^2} = \left(1 + \tau_o\frac{\partial}{\partial t}\right)$$
$$\left[\left(\rho C_e\frac{\partial^2 T}{\partial t^2} + T_o\left(\alpha_1\frac{\partial^3 u_1}{\partial t^2 \partial x_1} + \alpha_3\frac{\partial^3 u_3}{\partial t^2 \partial x_3}\right) - \frac{E_g}{\tau}\frac{\partial N}{\partial t}\right)\right], \tag{8}$$

$$D_1^*\frac{\partial^2 N}{\partial x_1^2} + D_3^*\frac{\partial^2 N}{\partial x_3^2} = \frac{\partial N}{\partial t} + \frac{N}{\tau} - \zeta\frac{T}{\tau}, \tag{9}$$

$$t_{33} = C_{13}\frac{\partial u_1}{\partial x_1} + C_{33}\frac{\partial u_3}{\partial x_3} - \alpha_3 T - \gamma_3 N, \tag{10}$$

$$t_{31} = C_{55}\left(\frac{\partial u_1}{\partial x_3} + \frac{\partial u_3}{\partial x_1}\right), \tag{11}$$

$$t_{11} = C_{11}\frac{\partial u_1}{\partial x_1} + C_{13}\frac{\partial u_3}{\partial x_3} - \alpha_1 T - \gamma_1 N. \tag{12}$$

where

$$\alpha_1 = C_{11}\alpha_1^* + C_{12}\alpha_2^* + C_{13}\alpha_3^*, \ \alpha_3 = C_{13}\alpha_1^* + C_{23}\alpha_2^* + C_{33}\alpha_3^*, \gamma_1 = C_{11}\gamma_1^* + C_{12}\gamma_2^* + C_{13}\gamma_3^*,$$
$$\gamma_3 = C_{13}\gamma_1^* + C_{23}\gamma_2^* + C_{33}\gamma_3^*.$$

α_1^*, α_2^* and α_3^* are linear thermal expansion coefficients, γ_1^*, γ_2^* and γ_3^* are electronic deformation coefficients, K_1, K_3 are thermal conductivity, K_1^*, K_3^* are thermal conductivity rate and D_1^* and D_3^* are carrier diffusion coefficients.

In the above equations we use the contracting subscript notations ($11\rightarrow 1, 22 \rightarrow 2, 33 \rightarrow 3, 23 \rightarrow 4, 31 \rightarrow 5, 12 \rightarrow 6$) to relate C_{ijkl} to C_{mn}. Also $K_{ij}\delta_{ij} = K_i, K_{ij}^*\delta_{ij} = K_i^*$ and $D_{ij}^*\delta_{ij} = D_i^*, i$ is not summed.

For non-dimensionalization of equations, following variables are taken

$$\left(x_1^{'}, x_3^{'}, u_1^{'}, u_3^{'}\right) = \eta_1 C_o(x_1, x_3, u_1, u_3) , \left(t_{11}^{'}, t_{33}^{'}, t_{31}^{'}\right) = \frac{1}{C_{11}}(t_{11}, t_{33}, t_{31}),$$
$$\left(t^{'}, \tau_o^{'}, \tau^{'}\right) = \eta_1 C_o^2(t, \tau_o, \tau) , T^{'} = \frac{\alpha_1 T}{\rho C_o^2}, \quad N^{'} = \frac{N}{n_o}, \tag{13}$$

also

$$\eta_1 = \frac{\rho C_e}{K_1}, C_o^2 = \frac{C_{11}}{\rho}.$$

Eqs. (6)-(12) reduced to the following form by taking into consideration Eq. (13) and after suppressing the prime as

$$\frac{\partial^2 u_1}{\partial x_1^2} + g_1\frac{\partial^2 u_1}{\partial x_3^2} + g_2\frac{\partial^2 u_3}{\partial x_1 \partial x_3} - \frac{\partial T}{\partial x_1} - g_3\frac{\partial N}{\partial x_1} = \frac{\partial^2 u_1}{\partial t^2}, \tag{14}$$

$$\frac{\partial^2 u_3}{\partial x_1^2} + g_4 \frac{\partial^2 u_3}{\partial x_3^2} + g_5 \frac{\partial^2 u_1}{\partial x_1 \partial x_3} - g_6 \frac{\partial T}{\partial x_3} - g_7 \frac{\partial N}{\partial x_3} = \frac{1}{g_1} \frac{\partial^2 u_3}{\partial t^2},$$

$$\frac{\partial^3 T}{\partial x_1^2 \partial t} + K^{**} \frac{\partial^3 T}{\partial x_3^2 \partial t} + g_{10} \frac{\partial^2 T}{\partial x_1^2} + g_{11} \frac{\partial^2 T}{\partial x_3^2} = \left(1 + \tau_o \frac{\partial}{\partial t}\right)$$

(15)

$$\left[g_{12} \frac{\partial^2 T}{\partial t^2} + g_{13} \frac{\partial^3 u_1}{\partial t^2 \partial x_1} + g_{14} \frac{\partial^3 u_3}{\partial t^2 \partial x_3} + \frac{g_{15}}{\tau} \frac{\partial N}{\partial t}\right],$$

(16)

$$\frac{\partial^2 N}{\partial x_1^2} + D^* \frac{\partial^2 N}{\partial x_3^2} = g_8 \frac{\partial N}{\partial t} + g_8 \frac{N}{\tau} - g_9 \frac{T}{\tau},$$

(17)

$$t_{33} = g_{16} \frac{\partial u_1}{\partial x_1} + g_{17} \frac{\partial u_3}{\partial x_3} - g_{18} T - g_{19} N,$$

(18)

$$t_{31} = g_1 \left(\frac{\partial u_1}{\partial x_3} + \frac{\partial u_3}{\partial x_1}\right),$$

(19)

$$t_{11} = \frac{\partial u_1}{\partial x_1} + g_{17} \frac{\partial u_3}{\partial x_3} - T - g_3 N.$$

(20)

where

$$g_1 = \frac{C_{55}}{C_{11}}, g_2 = \frac{C_{13} + C_{55}}{C_{11}}, g_3 = \frac{\gamma_1 n_o}{C_{11}}, g_4 = \frac{C_{33}}{C_{55}},$$

$$g_5 = \frac{C_{13} + C_{55}}{C_{55}}, g_6 = \frac{\alpha_3 C_{11}}{\alpha_1 C_{55}}, g_7 = \frac{\gamma_3 n_o}{C_{55}}, g_8 = \frac{1}{\eta_1 D_1^*},$$

$$g_9 = \frac{\zeta \rho C_o^2}{\alpha_1 D_1^* n_o \eta_1}, g_{10} = \frac{K_1^*}{K_1 \eta_1 C_o^2}, g_{11} = \frac{K_3^*}{K_1 \eta_1 C_o^2}, g_{12} = \frac{\rho C_e}{K_1 \eta_1},$$

$$g_{13} = \frac{T_o \alpha_1 \alpha_1}{K_1 \eta_1 C_{11}}, g_{14} = \frac{T_o \alpha_3 \alpha_1}{K_1 \eta_1 C_{11}}, g_{15} = -\frac{E_g n_o \alpha_1}{K_1 \eta_1 \rho C_o^2},$$

$$g_{16} = \frac{C_{13}}{C_{11}} g_{17} = \frac{C_{33}}{C_{11}}, g_{18} = \frac{\alpha_3}{\alpha_1}, g_{19} = \frac{\gamma_3 n_o}{C_{11}},$$

$$K^{**} = \frac{K_3}{K_1}, D^* = \frac{D_3^*}{D_1^*}$$

(21)

Define Laplace and Fourier Transform as

$$\overline{f}(x_1, x_3, p) = \int_0^\infty f(x_1, x_3, p) e^{-pt} dt,$$

(22)

$$\hat{f}(\xi, x_3, p) = \int_{-\infty}^\infty \bar{f}(x_1, x_3, p) e^{i\xi s_1} dx_1.$$

(23)

Applying Laplace and Fourier transforms defined by Eqs. (22)-(23) on Eqs. (14)-(20), the following equations are obtained

$$-\xi^2 \hat{u}_1 + g_1 \frac{d^2 \hat{u}_1}{dx_3^2} - g_2 i\xi \frac{d\hat{u}_3}{dx_3} + i\xi \hat{T} + i\xi g_3 \hat{N} = p^2 \hat{u}_1,$$

(24)

$$-\xi^2 \hat{u}_3 + g_4 \frac{d^2 \hat{u}_3}{dx_3^2} - g_5 i\xi \frac{d\hat{u}_1}{dx_3} - g_6 \frac{d\hat{T}}{dx_3} - g_7 \frac{d\hat{N}}{dx_3} = \frac{p^2}{g_1} \hat{u}_3,$$

(25)

$$\left(p^2 g_{12}\hat{T} - i\xi p^2 g_{13}\hat{u}_1 + p^2 g_{14}\frac{d\hat{u}_3}{dx_3} + \frac{pg_{15}}{\tau}\hat{N}\right), \tag{26}$$

$$-\xi^2 \hat{N} + D^* \frac{d^2\hat{N}}{dx_3^2} = g_8 p\hat{N} + g_8\frac{\hat{N}}{\tau} - g_9\frac{\hat{T}}{\tau}, \tag{27}$$

$$\hat{t}_{33} = -g_{16}i\xi\hat{u}_1 + g_{17}\frac{d\hat{u}_3}{dx_3} - g_{18}\hat{T} - g_{19}\hat{N}, \tag{28}$$

$$\hat{t}_{31} = g_1\left(\frac{d\hat{u}_1}{dx_3} - i\xi\hat{u}_3\right), \tag{29}$$

$$\hat{t}_{11} = -i\xi\hat{u}_1 + g_{17}\frac{d\hat{u}_3}{dx_3} - \hat{T} - g_3\hat{N}. \tag{30}$$

After some algebraic calculation of Eqs. (24)- (27), determine the following

$$(D^8 + R_1 D^6 + R_2 D^4 + R_3 D^2 + R_4)(\hat{u}_1, \hat{u}_3, \hat{T}, \hat{N}) = 0. \tag{31}$$

where

$$R_1 = -r_6 - r_{10} - r_{13} - r_{10} - r_2 r_5,$$
$$R_2 = r_1 r_6 + r_1 r_{10} + r_1 r_{13} + r_3 r_{11} + r_6 r_{10} + r_6 r_{13} + r_7 r_{12} + r_9 r_{14} +$$
$$r_{10} r_{13} + r_2 r_5 r_{10} - r_1 r_7 r_{12} + r_2 r_5 r_{13} - r_2 r_7 r_{11} - r_3 r_5 r_{12} - r_7 r_{12} r_{10} - r_9 r_8 r_{12},$$
$$R_3 = -r_1 r_6 r_{10} - r_1 r_6 r_{13} - r_3 r_6 r_{11} - r_1 r_9 r_{14} - r_1 r_{13} r_{10} - r_3 r_{11} r_{10}$$
$$- r_4 r_9 r_{11} - r_6 r_9 r_{14} - r_{13} r_6 r_{10} + r_1 r_7 r_{10} r_{12} + r_1 r_8 r_9 r_{12} - r_2 r_5 r_9 r_{14}$$
$$- r_2 r_5 r_{10} r_{13} + r_2 r_7 r_{10} r_{11} + r_2 r_8 r_9 r_{11} + r_3 r_5 r_{10} r_{12} + r_4 r_5 r_9 r_{12} \ ,$$
$$R_4 = r_1 r_6 r_9 r_{14} + r_1 r_6 r_{10} r_{11} + r_3 r_6 r_{10} r_{11} + r_4 r_6 r_9 r_{11} \ , \tag{32}$$

also

$$r_1 = \frac{\xi^2 + p^2}{g_1}, r_2 = \frac{-i\xi g_2}{g_1}, r_3 = \frac{-i\xi}{g_1}, r_4 = \frac{-i\xi g_3}{g_1},$$
$$r_5 = \frac{-i\xi g_5}{g_4}, r_6 = \frac{g_1\xi^2 + p^2}{g_1 g_4}, r_7 = -\frac{g_6}{g_4}, r_8 = -\frac{g_7}{g_4},$$
$$r_9 = \frac{g_9}{\tau D^*}, r_{10} = \frac{\xi^2\tau + g_8(p\tau + 1)}{\tau D^*}, r_{11} = \frac{-i\xi p^2 g_{13}(1 + p\tau_o)}{pK^{**} + g_{11}},$$
$$r_{12} = \frac{(1 + p\tau_o)p^2 g_{14}}{pK^{**} + g_{11}}, r_{13} = \frac{\xi^2(p + g_{10}) + p^2 g_{12}(1 + p\tau_o)}{pK^{**} + g_{11}},$$
$$r_{14} = \frac{pg_{15}(1 + p\tau_o)}{\tau(pK^{**} + g_{11})}. \tag{33}$$

The general solution of Eq. (31) is written as

$$(\hat{u}_1, \hat{u}_3, \hat{T}, \hat{N}) = \sum_{j=1}^{4}(1, \alpha_{1j}, \beta_{1j}, \gamma_{1j}) C_j \cosh m_j x_3 . \tag{34}$$

where $m_j (j = 1,2,3,4)$ are roots of $D^8 + R_1 D^6 + R_2 D^4 + R_3 D^2 + R_4 = 0$ and coupling parameters are

$$\alpha_{1j} = \sum_{j=1}^{4} \frac{R_9 m_j^5 + R_{10} m_j^3 + R_{11} m_j}{R_5 m_j^6 + R_6 m_j^4 + R_7 m_j^2 + R_8} , \tag{35}$$

$$\beta_{1j} = \sum_{j=1}^{4} \frac{R_{12}m_j^4 + R_{13}m_j^2 + R_{14}}{R_5 m_j^6 + R_6 m_j^4 + R_7 m_j^2 + R_8}, \tag{36}$$

$$\gamma_{1j} = \sum_{j=1}^{4} \frac{R_{15}m_j^2 + R_{16}}{R_5 m_j^6 + R_6 m_j^4 + R_7 m_j^2 + R_8} \tag{37}$$

where

$$R_5 = ch_j^2, R_6 = ch_j^2 r_6 - ch_j^2 r_{10} + ch_j sh_j r_7 r_{12},$$
$$R_7 = ch_j^3 r_6 r_{10} + ch_j^3 r_6 r_{13} + ch_j^3 r_9 r_{14} + ch_j^3 r_{10} r_{13} +$$
$$ch_j sh_j^2 r_7 r_{12} r_{10} + ch_j sh_j^2 r_8 r_9 r_{12} \ ,$$
$$R_8 = -ch_j^3 r_6 r_9 r_{14} - ch_j^3 r_6 r_{10} r_{13}, R_9 = r_5 ch_j^3,$$
$$R_{10} = -ch_j^3 r_5 r_{10} - ch_j^3 r_5 r_{13} + sh_j ch_j^2 r_7 r_{11},$$
$$R_{11} = ch_j^3 r_5 r_9 r_{14} + ch_j^3 r_5 r_{10} r_{13} - sh_j ch_j^2 r_7 r_{10} r_{11}$$
$$- sh_j ch_j^2 r_8 r_9 r_{11} \ , \tag{38}$$
$$R_{12} = -r_{11} ch_j^3 - sh_j ch_j^2 r_5 r_{12}, R_{13} = -ch_j^3 r_6 r_{11} - ch_j^3 r_{11} r_{10} + sh_j ch_j^3 r_5 r_{10} r_{12},$$
$$R_{14} = ch_j^3 r_6 r_{10} r_{11}, R_{15} = ch_j^3 r_{11} r_9 - sh_j ch_j^2 r_5 r_9 r_{12}, R_{16} = -ch_j^3 r_6 r_9 r_{11},$$
$$\text{and } ch_j = cosh \ m_j \ x_3 \ , j = 1,2,3,4.$$

Expressions for stress components are obtained with the aid of Eqs. (28), (29) and (34) as

$$\hat{t}_{33} = -g_{16} i\xi \sum_{j=1}^{4} C_j \ cosh \ m_j \ x_3 + g_{17} \sum_{j=1}^{4} \alpha_{1j} m_j C_j \ sinh \ m_j \ x_3$$
$$-g_{18} \sum_{j=1}^{4} \beta_{1j} C_j \ cosh \ m_j \ x_3 - g_{19} \sum_{j=1}^{4} \gamma_{1j} C_j \ cosh \ m_j \ x_3, \tag{39}$$

$$\hat{t}_{31} = g_1 \sum_{j=1}^{4} m_j C_j \ sinh \ m_j \ x_3 - i\xi g_1 \sum_{j=1}^{4} \alpha_{1j} C_j \ cosh \ m_j \ x_3. \tag{40}$$

4. Restrictions on the boundary

The boundary restrictions for an orthotropic photothermoelastic plate occupying the plane $x_3 = \pm d$ subjected to moving normal force, ramp type thermal source and carrier density source are considered as

$$\left.\begin{array}{l} t_{33} = -F_1(x_1, x_3, t), \\ t_{31} = 0, \\ T = F_2(x_1, t), \\ N = F_3(x_1, t), \end{array}\right\} \tag{41}$$

where

$$F_1(x_1, x_3, t) = F_{10} \delta(x_3 - vt) H(a - |x_1|), \tag{42}$$

$$F_2(x_1, t) = \delta(x_1) \begin{cases} 0 \; ; \; t \le 0, \\ F_{20}\dfrac{t}{t_o}; 0 \le t \le t_0, \\ F_{20}; t > t_o, \end{cases} \tag{43}$$

$$F_3(x_1, t) = F_{30}\delta(x_1) \sin b\, t. \tag{44}$$

also, $H(\ )$ is Heaviside step function, $\delta(\ )$ is Dirac delta function, v is the velocity, F_{10} is the magnitude of the force, F_{20} is the constant temperature applied on the boundary and F_{30} is constant.

Applying Laplace and Fourier transform defined by Eqs. (22)-(23) on Eqs. (41)-(44), we attain

$$\left.\begin{aligned} \hat{t}_{33} &= -\hat{F}_1(\xi, x_3, p), \\ \hat{t}_{31} &= 0, \\ \hat{T} &= \hat{F}_2(\xi, p), \\ \hat{N} &= \hat{F}_3(\xi, p), \end{aligned}\right\} \text{ at } x_3 = \pm d \tag{45}$$

where

$$\hat{F}_1(\xi, x_3, p) = \frac{F_{10}}{v} e^{\frac{-p}{v}x_3} \frac{2 \sin a\xi}{\xi}, \tag{46}$$

$$\hat{F}_2(\xi, p) = \frac{F_{20}(1-e^{-pt_o})}{t_0 p^2}, \tag{47}$$

$$\hat{F}_3(\xi, p) = F_{30}\frac{b}{(p^2+b^2)}. \tag{48}$$

Substituting the values of $\hat{t}_{33}, \hat{t}_{31}, \hat{T}$ and $\hat{N}$ from Eqs. (39)-(40) and (34) in the transformed boundary restrictions Eq. (45), along with Eqs. (46)-(48) yield

$$\sum_{j=1}^{4}(d_j C_j \cosh m_j x_3) = -\hat{F}_1(\xi, x_3, p), \tag{49}$$

$$\sum_{j=1}^{4}(\alpha_{1j} C_j \cosh m_j x_3) = 0, \tag{51}$$

$$\sum_{j=1}^{4}(\beta_{1j} C_j \cosh m_j x_3) = \hat{F}_2(\xi, p), \tag{51}$$

$$\sum_{j=1}^{4}(\gamma_{1j} C_j \cosh m_j x_3) = \hat{F}_3(\xi, p). \tag{52}$$

where $d_j = -g_{16}i\xi - g_{18}\beta_{1j} - g_{19}\gamma_{1j}$, $j = 1,2,3,4.$

Eqs. (49)-(52) are taken in matrix form as

$$AC=B, \tag{53}$$

where

$$A = \begin{bmatrix} d_1 ch_1 & d_2 ch_2 & d_3 ch_3 & d_4 ch_4 \\ \alpha_{11}ch_1 & \alpha_{12}ch_2 & \alpha_{13}ch_3 & \alpha_{14}ch_4 \\ \beta_{11}ch_1 & \beta_{12}ch_2 & \beta_{13}ch_3 & \beta_{14}ch_4 \\ \gamma_{11}ch_1 & \gamma_{12}ch_2 & \gamma_{13}ch_3 & \gamma_{14}ch_4 \end{bmatrix}, C = \begin{bmatrix} C_1 \\ C_2 \\ C_3 \\ C_4 \end{bmatrix}, B = \begin{bmatrix} -F_1(x_1, x_3, t) \\ 0 \\ F_2(x_1, t) \\ F_3(x_1, t) \end{bmatrix}, \tag{54}$$

From Eq. (54), we determine

$$C_j = \frac{\Delta_j}{\Delta}, j = 1,2,3,4 \tag{55}$$

where

$$\Delta = det\, A, \Delta_j = \text{determinant of } A \text{ when } j^{\text{th}} \text{ column of } A \text{ replaced by } B \text{ and} \tag{56}$$

$$
\begin{aligned}
\Delta = ch_1 ch_2 ch_3 ch_4 (&\beta_{11}\gamma_{14}d_2\alpha_{13} - \beta_{11}\gamma_{13}d_2\alpha_{14} + \\
&\beta_{11}\gamma_{12}d_3\alpha_{14} - \beta_{11}\gamma_{14}d_3\alpha_{12} - \beta_{11}\gamma_{12}d_4\alpha_{13} + \beta_{11}\gamma_{13}d_4\alpha_{12} \\
+&\beta_{12}\gamma_{13}d_1\alpha_{14} - \beta_{12}\gamma_{14}d_1\alpha_{13} - \beta_{12}\gamma_{11}d_3\alpha_{14} + \beta_{12}\gamma_{14}d_3\alpha_{11} \\
+&\beta_{12}\gamma_{11}d_4\alpha_{13} + \beta_{12}\gamma_{13}d_4\alpha_{11} - \beta_{13}\gamma_{11}d_4\alpha_{13} + \\
&\beta_{13}\gamma_{14}d_1\alpha_{12} + \beta_{13}\gamma_{11}d_2\alpha_{14} - \beta_{13}\gamma_{14}d_2\alpha_{11} - \beta_{13}\gamma_{11}d_4\alpha_{12} \\
+&\beta_{13}\gamma_{12}d_4\alpha_{11} + \beta_{14}\gamma_{12}d_1\alpha_{13} - \beta_{14}\gamma_{11}d_2\alpha_{13} \\
&-\beta_{14}\gamma_{13}d_2\alpha_{11} - \beta_{14}\gamma_{11}d_3\alpha_{12} - \beta_{14}\gamma_{12}d_3\alpha_{11}),
\end{aligned} \tag{57}
$$

$$\Delta_1 = -F_1 R_{17} + F_2 R_{18} - F_3 R_{19}, \tag{58}$$

$$\Delta_2 = F_1 R_{20} + F_2 R_{21} - F_3 R_{22}, \tag{59}$$

$$\Delta_3 = -F_1 R_{23} + F_2 R_{24} - F_3 R_{25}, \tag{60}$$

$$\Delta_4 = -F_1 R_{26} + F_2 R_{27} - F_3 R_{28}, \tag{61}$$

also

$$
\begin{aligned}
R_{17} = &\beta_{12}\gamma_{13}\alpha_{14}ch_2 ch_3 ch_4 + \beta_{12}\gamma_{14}\alpha_{13}ch_2 ch_3 ch_4 \\
&+ \beta_{13}\gamma_{12}\alpha_{14}ch_2 ch_3 ch_4 - \beta_{13}\gamma_{14}\alpha_{12}ch_2 ch_3 ch_4 \\
&- \beta_{14}\gamma_{12}\alpha_{13}ch_2 ch_3 ch_4 + \beta_{14}\gamma_{13}\alpha_{12}ch_2 ch_3 ch_4 \;, \\
R_{18} = &-\gamma_{13}\alpha_{14}ch_2 ch_3 ch_4 + \gamma_{14}\alpha_{13}ch_2 ch_3 ch_4 \\
&+\gamma_{12}\alpha_{14}ch_2 ch_3 ch_4 - \gamma_{14}\alpha_{12}ch_2 ch_3 ch_4 \\
&+\gamma_{12}\alpha_{13}ch_2 ch_3 ch_4 + \gamma_{13}\alpha_{12}ch_2 ch_3 ch_4, \\
R_{19} = &\beta_{12}d_4\alpha_{13}ch_2 ch_3 ch_4 - \beta_{12}d_3\alpha_{14}ch_2 ch_3 ch_4 \\
&+\beta_{13}d_2\alpha_{14}ch_2 ch_3 ch_4 - \beta_{13}d_4\alpha_{12}ch_2 ch_3 ch_4 \\
&-\beta_{14}d_2\alpha_{13}ch_2 ch_3 ch_4 + \beta_{14}d_3\alpha_{12}ch_2 ch_3 ch_4, \\
R_{20} = &\beta_{12}\gamma_{13}\alpha_{14}ch_1 ch_3 ch_4 - \beta_{11}\gamma_{14}\alpha_{13}ch_1 ch_3 ch_4 \\
&-\beta_{13}\gamma_{11}\alpha_{14}ch_1 ch_3 ch_4 + \beta_{13}\gamma_{14}\alpha_{11}ch_1 ch_3 ch_4 + \\
&\beta_{14}\gamma_{11}\alpha_{13}ch_1 ch_3 ch_4 - \beta_{14}\gamma_{13}\alpha_{11}ch_1 ch_3 ch_4, \\
R_{21} = &d_1\gamma_{13}\alpha_{14}ch_1 ch_3 ch_4 + d_1\gamma_{14}\alpha_{13}ch_1 ch_3 ch_4 \\
&-d_3\gamma_{14}\alpha_{14}ch_1 ch_3 ch_4 + d_3\gamma_{14}\alpha_{11}ch_1 ch_3 ch_4 \\
&+d_4\gamma_{11}\alpha_{13}ch_1 ch_3 ch_4 - d_4\gamma_{13}\alpha_{11}ch_1 ch_3 ch_4, \\
R_{22} = &d_3\beta_{11}\alpha_{14}ch_1 ch_3 ch_4 - d_4\beta_{11}\alpha_{13}ch_1 ch_3 ch_4 \\
&-d_4\beta_{13}\alpha_{11}ch_1 ch_3 ch_4 + d_1\beta_{13}\alpha_{14}ch_1 ch_3 ch_4 + \\
&d_1\beta_{14}\alpha_{13}ch_1 ch_3 ch_4 - d_3\beta_{14}\alpha_{11}ch_1 ch_3 ch_4, \\
R_{23} = &\beta_{11}\gamma_{12}\alpha_{14}ch_1 ch_2 ch_4 + \beta_{11}\gamma_{14}\alpha_{12}ch_1 ch_2 ch_4 \\
&+\beta_{12}\gamma_{11}\alpha_{14}ch_1 ch_2 ch_4 - \beta_{12}\gamma_{14}\alpha_{11}ch_1 ch_2 ch_4 - \\
&\beta_{14}\gamma_{11}\alpha_{12}ch_1 ch_2 ch_4 + \beta_{14}\gamma_{12}\alpha_{11}ch_1 ch_2 ch_4, \\
R_{24} = &d_1\gamma_{12}\alpha_{14}ch_1 ch_2 ch_4 + d_1\gamma_{14}\alpha_{12}ch_1 ch_2 ch_4 \\
&+d_2\gamma_{11}\alpha_{14}ch_1 ch_2 ch_4 - d_2\gamma_{14}\alpha_{11}ch_1 ch_2 ch_4 \\
&-d_4\gamma_{11}\alpha_{12}ch_1 ch_2 ch_4 + d_4\gamma_{12}\alpha_{11}ch_1 ch_2 ch_4,
\end{aligned}
$$

$$
\begin{aligned}
R_{25} &= d_4\beta_{11}\alpha_{12}ch_1ch_2ch_4 - d_2\beta_{11}\alpha_{14}ch_1ch_2ch_4 \\
&+ d_1\beta_{12}\alpha_{14}ch_1ch_2ch_4 - d_4\beta_{12}\alpha_{11}ch_1ch_2ch_4 - \\
&\quad d_1\beta_{14}\alpha_{12}ch_1ch_2ch_4 + d_2\beta_{14}\alpha_{11}ch_1ch_2ch_4, \\
R_{26`} &= \beta_{11}\gamma_{12}\alpha_{13}ch_1ch_2ch_3 - \beta_{11}\gamma_{13}\alpha_{12}ch_1ch_2ch_3 \\
&- \beta_{12}\gamma_{11}\alpha_{13}ch_1ch_2ch_3 + \beta_{12}\gamma_{13}\alpha_{11}ch_1ch_2ch_3 + \\
&\beta_{13}\gamma_{11}\alpha_{12}ch_1ch_2ch_3 + \beta_{13}\gamma_{12}\alpha_{11}ch_1ch_2ch_3, \\
R_{27} &= d_1\gamma_{12}\alpha_{13}ch_1ch_2ch_3 - d_1\gamma_{13}\alpha_{12}ch_1ch_2ch_3 - \\
&d_2\gamma_{11}\alpha_{13}ch_1ch_2ch_3 + d_2\gamma_{13}\alpha_{11}ch_1ch_2ch_3 \\
&+ d_3\gamma_{11}\alpha_{12}ch_1ch_2ch_3 - d_3\gamma_{12}\alpha_{11}ch_1ch_2ch_3 \ , \\
R_{28} &= d_2\beta_{11}\alpha_{13}ch_1ch_2ch_3 - d_3\beta_{11}\alpha_{12}ch_1ch_2ch_3 \\
&- d_1\beta_{12}\alpha_{13}ch_1ch_2ch_3 + d_3\beta_{12}\alpha_{11}ch_1ch_2ch_3 + \\
&d_1\beta_{13}\alpha_{12}ch_1ch_2ch_4 - d_2\beta_{13}\alpha_{11}ch_1ch_2ch_3.
\end{aligned}
\tag{62}
$$

Substituting the values of C_j from Eq. (55) in Eq. (34) and Eqs. (39)-(40), determine the displacement components, stress components, temperature distribution and carrier density distribution as

$$
\hat{u}_1 = \frac{1}{\Delta}\Big(L_1\hat{F}_1(\xi,p) + L_2\hat{F}_2(\xi,p) + L_3\hat{F}_3(\xi,p)\Big),
\tag{63}
$$

$$
\hat{u}_3 = \frac{1}{\Delta}\Big(L_4\hat{F}_1(\xi,p) + L_5\hat{F}_2(\xi,p) + L_6\hat{F}_3(\xi,p)\Big),
\tag{64}
$$

$$
\hat{t}_{33} = \frac{1}{\Delta}\Big(L_{13}\hat{F}_1(\xi,p) + L_{14}\hat{F}_2(\xi,p) + L_{15}\hat{F}_3(\xi,p)\Big),
\tag{65}
$$

$$
\hat{t}_{31} = \frac{1}{\Delta}\Big(L_{16}\hat{F}_1(\xi,p) + L_{17}\hat{F}_2(\xi,p) + L_{18}\hat{F}_3(\xi,p)\Big),
\tag{66}
$$

$$
\hat{T} = \frac{1}{\Delta}\Big(L_7\hat{F}_1(\xi,p) + L_8\hat{F}_2(\xi,p) + L_9\hat{F}_3(\xi,p)\Big),
\tag{67}
$$

$$
\hat{N} = \frac{1}{\Delta}\Big(L_{10}\hat{F}_1(\xi,p) + L_{11}\hat{F}_2(\xi,p) + L_{12}\hat{F}_3(\xi,p)\Big).
\tag{68}
$$

where

$$
\begin{aligned}
L_1 &= R_{17}ch_1 - R_{20}ch_2 - R_{23}ch_3 - R_{26}ch_4 \ , \\
L_2 &= R_{18}ch_1 + R_{21}ch_2 + R_{24}ch_3 - R_{27}ch_4, \\
L_3 &= -R_{19}ch_1 - R_{22}ch_2 - R_{25}ch_3 - R_{28}ch_4 \ , \\
L_4 &= R_{17}ch_1\alpha_{11} - R_{20}ch_2\alpha_{12} - R_{23}ch_3\alpha_{13} - R_{26}ch_4\alpha_{14}, \\
L_5 &= R_{18}ch_1\alpha_{11} - R_{21}ch_2\alpha_{12} - R_{24}ch_3\alpha_{13} - R_{27}ch_4\alpha_{14} \ , \\
L_6 &= R_{19}ch_1\alpha_{11} - R_{22}ch_2\alpha_{12} - R_{25}ch_3\alpha_{13} - R_{28}ch_4\alpha_{14}, \\
L_7 &= R_{17}d_1 - g_{18}ch_1\beta_{11} - R_{20}d_2 + g_{18}ch_2\beta_{12} - R_{23}d_3 \\
&+ g_{18}ch_3\beta_{13} - R_{26}d_4 + g_{18}ch_4\beta_{14} \ , \\
L_8 &= R_{18}d_1 - g_{18}ch_1\beta_{11} + R_{21}d_2 - g_{18}ch_2\beta_{12} + R_{24}d_3 \\
&- g_{18}ch_3\beta_{13} + R_{27}d_4 - g_{18}ch_4\beta_{14}, \\
L_9 &= -R_{19}d_1 + g_{18}ch_1\beta_{11} - R_{22}d_2 + g_{18}ch_2\beta_{12} - R_{25}d_3 \\
&+ g_{18}ch_3\beta_{13} - R_{28}d_4 + g_{18}ch_4\beta_{14},
\end{aligned}
$$

$$L_{10} = g_1 m_1 R_{17} ch_1 - i\xi g_1 \alpha_{11} R_{17} sh_1 - g_1 m_2 R_{20} ch_2$$
$$+ i\xi g_1 \alpha_{12} R_{20} sh_2 - g_1 m_3 R_{23} ch_3 + i\xi g_1 \alpha_{14} R_{23} sh_3$$
$$- g_1 m_4 R_{26} ch_4 + i\xi g_1 \alpha_{14} R_{26} sh_4,$$
$$L_{11} = g_1 m_1 R_{18} ch_1 - i\xi g_1 \alpha_{11} R_{18} sh_1 + g_1 m_2 R_{21} ch_2$$
$$+ i\xi g_1 \beta_{12} R_{21} sh_2 - g_1 m_3 R_{24} ch_3 + i\xi g_1 \beta_{14} R_{24} sh_4$$
$$- g_1 m_4 R_{27} ch_3 + i\xi g_1 \beta_{14} R_{27} sh_4 ,$$
$$L_{12} = g_1 m_1 R_{19} ch_1 - i\xi g_1 \alpha_{11} R_{19} sh_1 + g_1 m_2 R_{22} ch_2 +$$
$$i\xi g_1 \alpha_{12} R_{22} sh_2 - g_1 m_3 R_{25} ch_3 + i\xi g_1 \alpha_{14} R_{25} sh_4$$
$$- g_1 m_4 R_{28} ch_3 + i\xi g_1 \alpha_{14} R_{28} sh_4,$$
$$L_{13} = \beta_{11} R_{17} ch_1 - \beta_{12} R_{20} ch_2 - \beta_{13} R_{23} ch_3 - \beta_{14} R_{26} ch_4 ,$$
$$L_{14} = \beta_{11} R_{18} ch_1 + \beta_{12} R_{21} ch_2 + \beta_{13} R_{24} ch_3 + \beta_{14} R_{27} ch_4,$$
$$L_{15} = -\beta_{11} R_{19} ch_1 - \beta_{12} R_{22} ch_2 - \beta_{13} R_{25} ch_3 - \beta_{14} R_{28} ch_4 ,$$
$$L_{16} = \gamma_{11} R_{17} ch_1 - \gamma_{12} R_{20} ch_2 - \gamma_{13} R_{23} ch_3 - \gamma_{14} R_{26} ch_4,$$
$$L_{17} = \gamma_{11} R_{18} ch_1 + \gamma_{12} R_{21} ch_2 + \gamma_{13} R_{24} ch_3 + \gamma_{14} R_{27} ch_4 ,$$

$$L_{18} = -\gamma_{11} R_{19} ch_1 - \gamma_{12} R_{22} ch_2 - \gamma_{13} R_{25} ch_3 - \gamma_{14} R_{28} ch_4. \qquad (69)$$

5. Particular cases

(i) For moving normal force $F_{20} = F_{30} = 0$ yield

$$\left(\hat{u}_1, \hat{u}_3, \hat{t}_{33}, \hat{t}_{31}, \hat{T}, \hat{N}\right) = \frac{1}{\Delta}\left((L_1, L_4, L_{13}, L_{16}, L_7, L_{10})\hat{F}_1(\xi, x_3, p)\right), \qquad (70)$$

where $\hat{F}_1(\xi, x_3, p)$ is given by Eq. (46)

(ii) For ramp type thermal Source $F_{10} = F_{30} = 0$ yield

$$\left(\hat{u}_1, \hat{u}_3, \hat{t}_{33}, \hat{t}_{31}, \hat{T}, \hat{N}\right) = \frac{1}{\Delta}\left((L_2, L_5, L_{14}, L_{17}, L_8, L_{11})\hat{F}_2(\xi, p)\right), \qquad (71)$$

where $\hat{F}_2(\xi, p)$ is given by Eq. (47)

(iii) For carrier density source $F_{10} = F_{20} = 0$ yield

$$\left(\hat{u}_1, \hat{u}_3, \hat{t}_{33}, \hat{t}_{31}, \hat{T}, \hat{N}\right) = \frac{1}{\Delta}\left((L_3, L_6, L_{15}, L_{18}, L_9, L_{12})\hat{F}_3(\xi, p)\right), \qquad (72)$$

where $\hat{F}_3(\xi, p)$ is given by Eq. (48)

(iv) Taking $\tau_o = K_1^* = K_3^* = 0$ in Eqs. (63)-(68) yield the desired expressions for Classical thermoelastic CTE) model and the results are similar as obtained by Kumar *et al.* (2022) in a particular case.

(v) Considering $K_1^* = K_3^* = 0$ in Eqs. (63)-(68) determine the related quantities for Lord and Shulman's (LS) model. These results are in agreement with those obtained by Kumar *et al.* (2022) in a special case.

(vi) Allowing $\tau_o = K_1 = K_3 = 0$ in Eqs. (63)-(68) yield the corresponding expressions for Green and Naghdi of type-II (GN-II) model.

(vii) Considering $\tau_o = 0$ in Eqs. (63)-(68) determine the related expressions for Green and Naghdi of type- III (GN-III) model .

6. Unique cases

a) If $C_{11} = C_{33} = \lambda + 2\mu, C_{13} = \lambda, C_{55} = \mu, \ \alpha_{1t} = \alpha_{3t} = \alpha_t, \gamma_{1d} = \gamma_{3d} = \gamma_n, D_1 = D_3 = D_e$, $K_1 = K_3 = K$ and $K_1^* = K_3^* = K^*$ in Eqs. (63)-(68), then all corresponding results are obtained for isotropic photothermoelastic plate under Moore-Gibson-Thompson thermoelastic model.
b) In absence of carrier density parameter (*N*=0) in Eqs. (63)-(68), we obtain the corresponding expressions for $\hat{u}_1, \hat{u}_3$ and $\hat{T}$ for thermoelastic plate under Moore-Gibson-Thompson model, as where m_1, m_2, m_3 be the roots of characteristic equation

$$D^6 + R_{29}D^4 + R_{30}D^2 + R_{31} = 0,$$

$$\left(\hat{u}_1, \hat{u}_3, \hat{T}\right) = \sum_{j=1}^{3}\left(1, a_j, b_j\right) C_j \cosh m_j x_3, \tag{77}$$

The coupling parameters are as

$$a_j = \sum_{j=1}^{3}\frac{R_{35}m_j^3 + R_{36}m_j}{R_{32}m_j^4 + R_{33}m_j^2 + R_{34}}, \text{ and } \ b_j = \sum_{j=1}^{3}\frac{R_{37}m_j^2 + R_{38}}{R_{32}m_j^4 + R_{33}m_j^2 + R_{34}}.$$

7. Numerical results and discussion

For the numerical calculations, we take material constants for orthotropic Silicon (Si) material as

$$C_{11} = 19.45 \text{ N/m}^2, C_{13} = 6.41 \text{ N/m}^2, C_{33} = 16.57 \text{ N/m}^2, C_{55} = 7.96 \text{ N/m}^2,$$
$$\alpha_{1t} = 3.25 \text{ N/m}^2\text{K}, \alpha_{3t} = 3.10 \text{ N/m}^2\text{K}, \gamma_{1d} = -0.029715 \text{ m}^3, \gamma_{3d} = -0.02714 \text{ m}^3,$$
$$\rho = 2328 \text{ kg/m}^3, T_o = 300 \text{ K}, T_p = 2 \text{ ps}, K_1 = 192 \text{ w/mk}, K_3 = 190 \text{ w/mk}, E_g = 1.11eV,$$
$$C_e = 710 \, j/kg \, K, \tau = 5s, D_1^* = 4.0 \, m^2/s, D_3^* = 3.5 \, m^2/s, n_o = 10^{20}m^{-3}.$$

For MGTE the following cases are taken into account:
(i) Moving normal force $F_{20} = F_{30} = 0 \, for \, v = 0.1, 0.2, 0.4$.
(ii) Ramp type thermal source $F_{10} = F_{30} = 0 \, for \, t_o = 0.1, 0.2, 0.3$.
(iii) Carrier Density source $F_{10} = F_{20} = 0 \, for \, b = 0.1, 0.3, 0.5$.
Case-I: Figs. 1.1-1.9 depict the variations of all field variables with plate length x_1 on the plane $x_3 = 1$ for the different theories of photothermpelasticity.
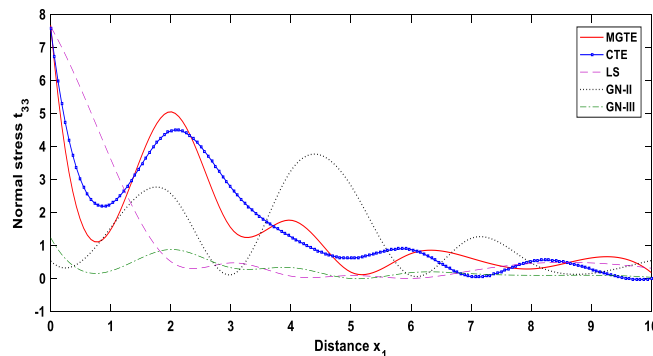

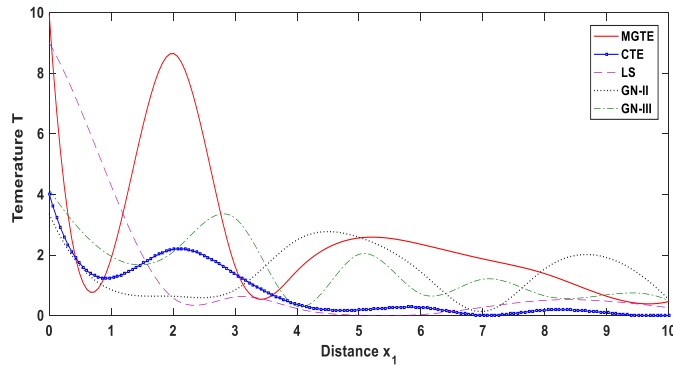Fig. 1.1 Profile of t_{33} vs x_1 (MNF)
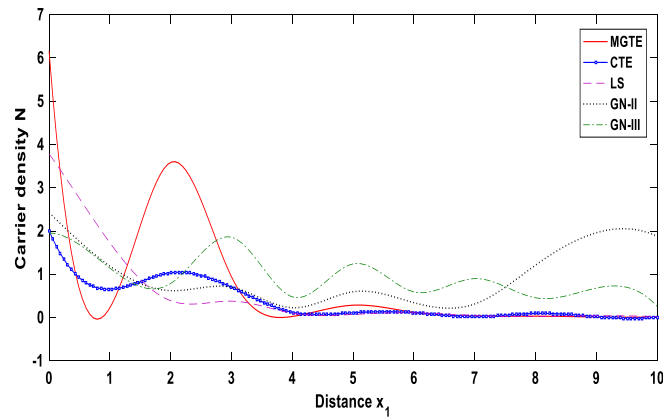
Fig. 1.2 Profile of *T* vs x_1 (MNF)

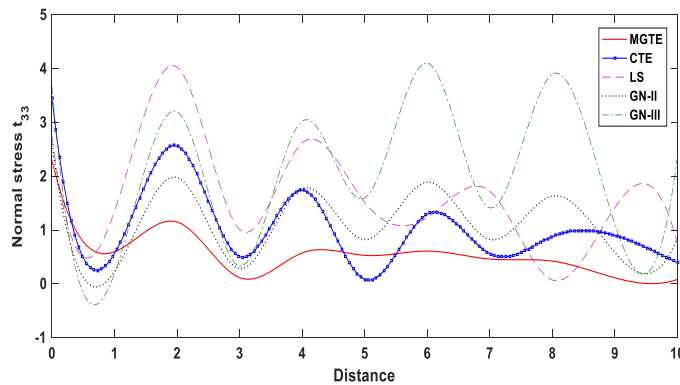Fig. 1.3 Profile of *N* vs x_1 (MNF)

Fig. 1.4 Profile of t_{33} vs x_1 (RTS)

Figs. 1.1-1.3 represent moving normal force (MNF), Figs. 1.4-1.6 represents ramp type thermal source (RTS), Figs. 1.7-1.9 represent carrier density source (CDS). In all the figures solid line correspond to photothermoelastic Moore-Gibson-Thompson (MGTE) model, Solid line with center symbol square corresponds to classical thermoelastic (CTE) model, dashed line corresponds
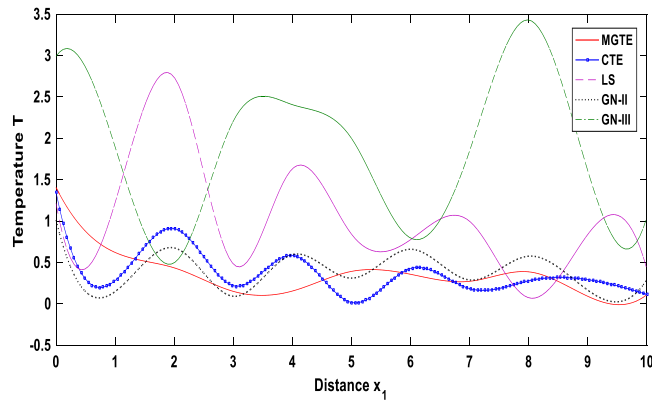
Fig. 1.5 Profile of T vs x_1 (RTS)
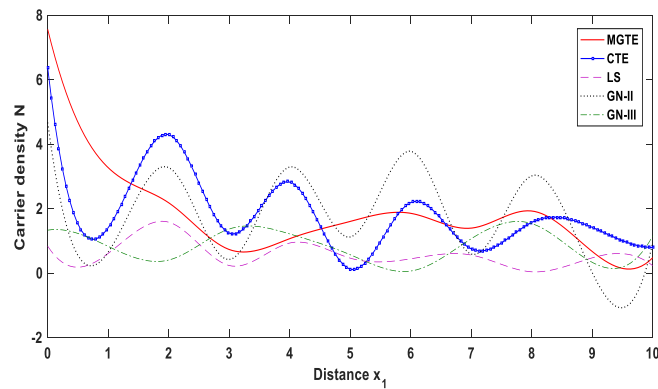
Fig. 1.6 Profile of N vs x_1 (RTS)
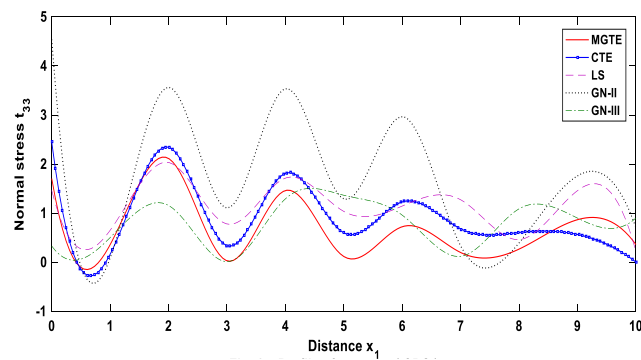
Fig. 1.7 Profile of t_{33} vs x_1 (CDS)

to Lord and Shulman (LS) model, dotted line corresponds to Green and Naghdi type-II (GN-II) model and dash-dot line corresponds to Green and Naghdi of type-III (GN-III) model.

Moving normal force (MNF),
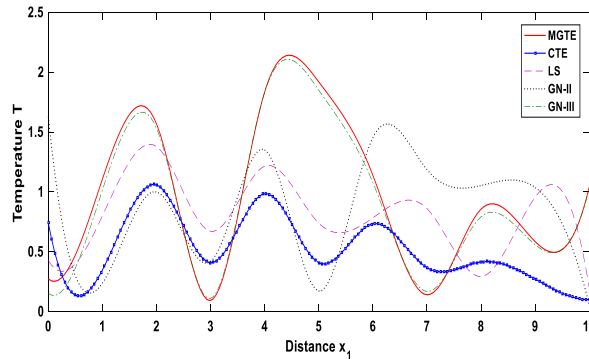Fig. 1.1 depicts trend of normal stress t_{33} vs. x_1. Near the source, the magnitude of t_{33} is
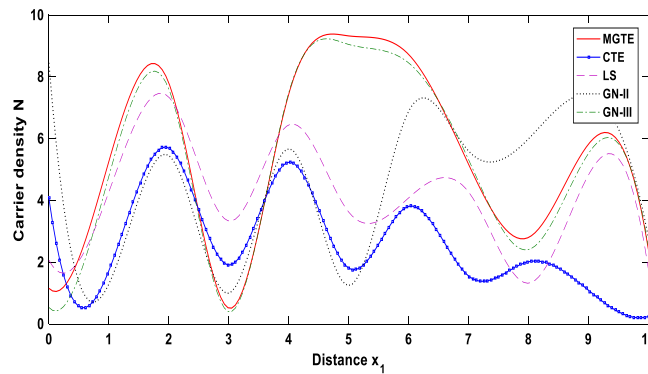
Fig. 1.8 Profile of T vs x_1 (CDS)

Fig. 1.9 Profile of N vs x_1 (CDS)

higher for LS model as compare to other models. The behavior and variation of t_{33} is opposite oscillatory for MGTE and CTE models, in some finite domain. Away from the source, all the curves correspond to t_{33} be converges for all models except GN-II.

Fig. 1.2 displays trend of temperature distribution T vs. x_1. Near the source, the magnitude of T is maximum for MGTE model and minimum for GN-II model. Away from source, all the curves correspond to T be converges for all models except MGTE model. The curve due to LS model is monotonically decreasing in the range $0 \leq x_1 \leq 2$. All the curves correspond to T are oscillating in nature for MGTE, CTE, LS and GN-II and GN-II models.

Fig. 1.3 demonstrates trend of carrier density distribution N vs x_1. Near the source, MGTE model enhances the magnitude of N as compare to other models. The curves correspond to N for CTE, LS and MGTE model behave almost similar with minor difference in their magnitude, in the range $4 \leq x_1 \leq 10$.

Ramp type thermal source (RTS),

Fig. 1.4 shows trend of normal stress t_{33} vs. x_1. Near the source magnitude of t_{33} is higher due to one relaxation time, whereas MGTE decreases the value of t_{33}. The curves correspond to t_{33} for GN-II and LS model are opposite oscillatory in the range $5 \leq x_1 \leq 10$. Away from source, the curves correspond to t_{33} be converges for LS and CTE model. GN-III model enhances the magnitude of t_{33} for the intermediate values of x_1.
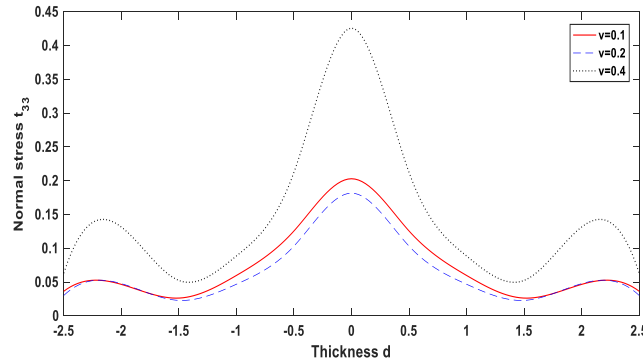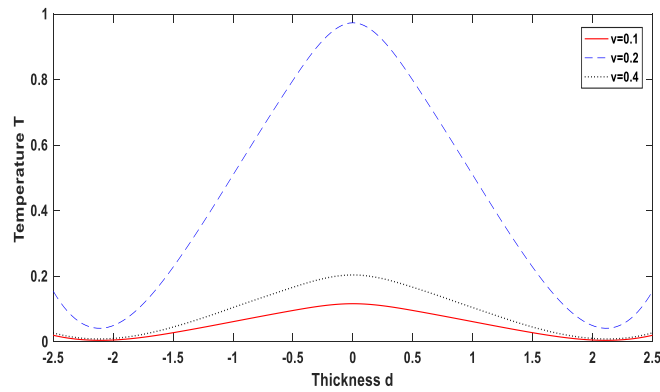
Fig. 1.10 Profile of t_{33} vs d (MNF)

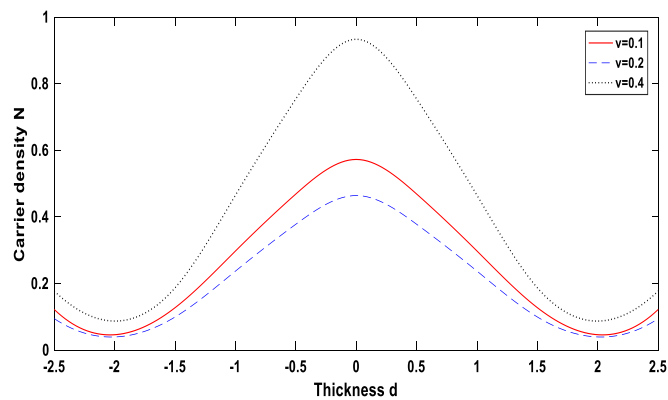Fig. 1.11 Profile of T vs d (MNF)

Fig. 1.12 Profile of N vs d (MNF)

Fig. 1.5 depicts trend of temperature distribution T vs. x_1. Near the source, the magnitude of T is increases in the presence of energy dissipation, whereas T attains minimum value in absence of energy dissipation. The curve correspond to T due to MGTE is less oscillatory as compare to other models. The curves due to LS and GN-II are opposite oscillatory in some finite domain. The
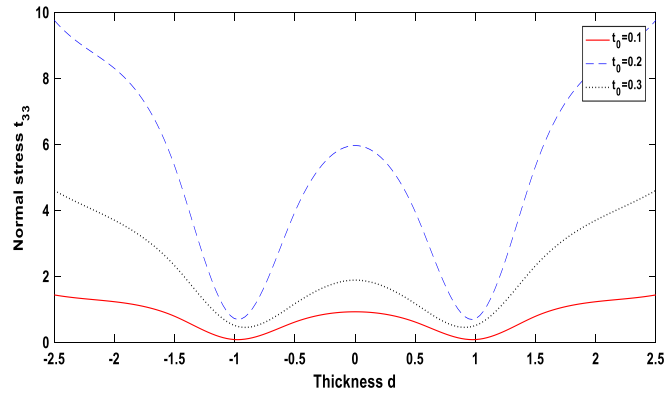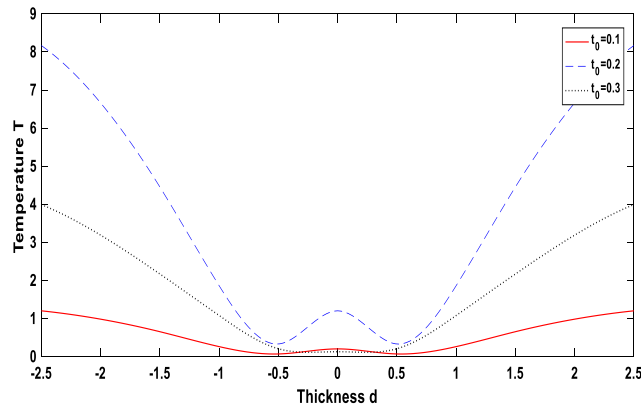
Fig. 1.13 Profile of t_{33} vs d (RTS)

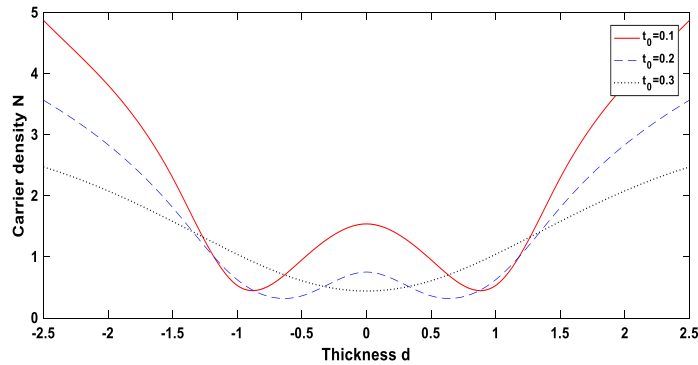Fig. 1.14 Profile of T vs d (RTS)

Fig. 1.15 Profile of N vs d (RTS)

curves for CTE and GN-II behave almost similar.

Fig. 1.6 shows trend of carrier density distribution N vs. x_1. Near the source, the values of N increases for MGTE model and decreases due to one relaxation time. The curves correspond to N behave almost similar for CTE and GN-II models in the finite domain of x_1. Away from source,
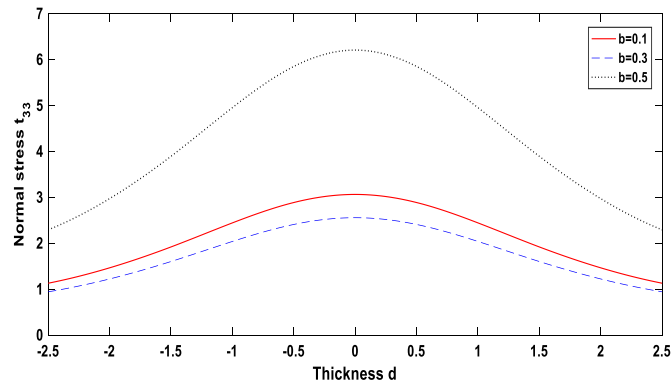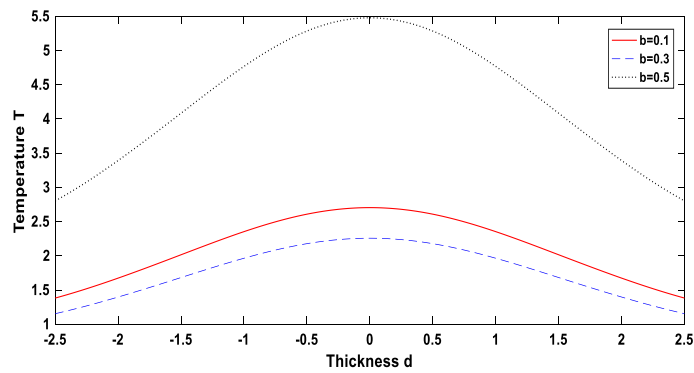
Fig. 1.16 Profile of t_{33} vs d (CDS)
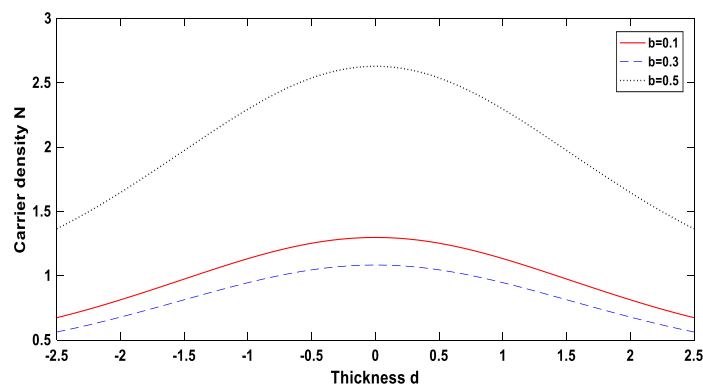

Fig. 1.17 Profile of T vs d (CDS)

Fig. 1.18 Profile of N vs d (CDS)

the curves correspond to N be converges for LS and CTE model. The curve due to GN-III and LS model are opposite oscillatory.

Carrier density source (CDS),
Fig. 1.7 depicts trend of normal stress t_{33} vs. x_1. Initially, the value of t_{33} is maximum due to

GN-II model and minimum due to GN-III model. Away from source, all the curves correspond to t_{33} be converges except GN-III model. The curves correspond to t_{33} for CTE model lies between MGTE and LS model for the intermediate values of x_1.

Fig. 1.8 demonstrates trend of T vs. x_1. Near the source, the magnitude of T is higher in the absence of energy dissipation, whereas presence of energy dissipation decreases the value of T. The curves correspond to T are opposite oscillatory due to LS and MGTE models, in some finite domain. The curve for CTE model lies in between LS model and GN-II model for the intermediate values of x_1.

Fig. 1.9 shows trend of carrier density N vs. x_1. Near the source the magnitude of N is higher due to GN-II model and minimum for GN-III model. All the curves correspond to N have fluctuating behavior for all the models. Away from source, all the curves due to MGTE, LS, GN-II and GN-III are converges except CTE model. Behavior and variation of curves are oscillatory for all the models.

Case-II: Figs. 1.10-1.18 depict the variations of all field variables with plate thickness d on the plane $x_1 = 1$ for different values of velocity, ramp type parameter and periodic parameter.

Figs. 1.10-1.12 represent moving normal force under MGTE with solid line, Figs. 1.13-1.15 represent ramp type thermal source under MGTE with dashed line, and Figs. 1.16-1.18 represent carrier density source under MGTE with dotted line.

Moving normal force under MGTE for different values of velocity v:

Fig. 1.10 depicts trend of normal stress t_{33} vs d. The magnitude of t_{33} is maximum when v=0.4 and minimum when v=0.2 at the middle point of the plate. The behavior and variation of t_{33} is similar for v= 0.1 and v= 0.2. t_{33} attain decreasing trend near the edges.

Fig. 1.11 displays the trend of temperature distribution T vs d. The magnitude of T remains higher when v=0.2 and lower when v=0.1 at the middle point of the plate. Behavior and variation of curves correspond to T is similar for v=0.1 and v=0.4. All the curves attain increasing trend near the edges, for all values of velocity v.

Fig. 1.12 shows the behavior of carrier density N vs. d. The magnitude of N is maximum at the middle point of the plate when v=0.4. A parabolic curve correspond to N is noticed at the middle point of the plate for all values of velocity. All the curves for all values of velocity v, attain increasing trend near the edges.

Ramp type thermal source (RTS) under MGTE for different values of ramp type parameter t_o:

Fig. 1.13 demonstrate the trend of normal stress t_{33} vs d. t_{33} attains maximum magnitude at (d=-2.5 and d=2.5) when t_o=0.2. All the curves correspond to t_{33} for different values of ramp type parameter are fluctuating in nature and attain increasing trend near the edges. A bell shaped curve is observed for N at the middle point of the plate when t_o=0.2.

Fig. 1.14 depicts the trend of temperature distribution T vs d. t_o=0.2 enhances the magnitude of T at (d=-2.5 and d=2.5) when t_o=0.2, whereas T attain the lowest magnitude when t_o=0.1. All the curves correspond to T for all values of t_o attain increasing trend near edges.

Fig. 1.15 displays the trend of carrier density N vs. d. t_o=0.1 enhances the magnitude of N at (d=-2.5 and d=2.5). Near the edges, the values of N due to t_o=0.2 lies between t_o=0.1 and t_o=0.3.

Carrier density source (CDS) under MGTE for different values of periodic parameter b:

Fig. 1.16 demonstrates trend of normal stress t_{33} vs d. The magnitude of t_{33} is maximum

when periodic parameter b=0.5 at the middle point of the plate. The behavior and variation of curves correspond to t_{33} remains similar for b=0.1 and b=0.3 with minimum difference of their magnitude.

Fig. 1.17 shows the trend of temperature distribution T vs d. The magnitude of T is maximum for b=0.5. All the curves correspond to T for all values of periodic parameter attain decreasing trend near the edges.

Fig. 1.18 depicts the trend of carrier density N vs d. The magnitude of N remains maximum when b=0.5 and minimum when b=0.3 at the middle point of the plate. The curves correspond to N are same in behavior and variation for b=0.1 and b=0.3.

8. Conclusions

In this paper a new model on Moore-Gibson-Thompson photothermoelastic theory has been established. Laplace and Fourier transform are used to solve the problem. Specific types of sources are taken to demonstrate the utility of the problem. The transformed expressions are converted into the physical domain by using numerical technique and presented in the form of figures. As the governing equations involved in this manuscript are of wave type, so the transfer of energy is done in the form of waves. After the numerical results the following conclusions are made:

t_{33} attain maximum magnitude for LS model, whereas MGTE model enhances the magnitude of T and N due to MNF. The behavior of t_{33}, T and N is oscillatory for all the assumed models. The impact of CTE model is more on t_{33} as compare to other models due to RTS. Behavior and variation of T and N are similar with distinct magnitude due to ramp type thermal source for all the theories. t_{33}, T and N attain maximum magnitude in absence of energy dissipation and minimum value in presence of energy dissipation in case of CDS.

Behavior of T and N are similar with velocity variations and with distinct magnitude, whereas t_{33} behave differently for MNF w.r.t. thickness of the plate. Magnitude of N gets decreases as ramp type parameter increases, whereas t_{33} and T get decreases for lowest ramp type parameter due to RTS in case of plate thickness. Variation and behavior of t_{33}, T and N are similar for periodic source parameter, magnitude of all parameters increases due to highest value of periodic source parameter for CDS w.r.t. thickness of the plate.

Due to MNF, RTS and CDS wave type behavior is observed for all the field variables depicting the significance of mechanical, thermal and carrier density response. MNF display a symmetric behavior for finite domain around the middle point of the plate. Away from middle point of the plate due to RTS depicts the decreasing and increasing behavior although in a small region symmetric tendency is observed. Smooth behavior is observed for near and away from the middle of the plate due to CDS.

It is concluded that normal stress, temperature distribution and carrier density distribution show a fluctuating behavior in presence of MGTE, CTE, LS, GN-II and GN-III model. Non-uniform pattern of curves is followed by the resulting quantities for moving normal force, ramp type thermal source and carrier density source with respect to length and thickness of the plate. Since the equations are coupled, arrival of the wave front at any point affects all the considered physical quantities. The finite speed of propagation manifests itself in all the figures. From the graphical representation there are three wave fronts (mechanical, thermal and carrier density response). The model described in this study may be used to design various semiconductor elements to meet special engineering requirements.

Acknowledgement

References

Abbas, I.A. (2011), "A two-dimensional problem for a fibre-reinforced anisotropic thermoelastic half-space with energy dissipation", *Sadhana*, **36**(3), 411-423. https://doi.org/10.1007/s12046-011-0025-5.

Abbas, I.A. (2014a), "Analytical solution for a free vibration of a thermoelastic hollow sphere", *Mech. Bas. Des. Struct. Mach.*, **43**(3), 265-276. https://doi.org/10.1080/15397734.2014.956244.

Abbas, I.A. (2014b), "Fractional order GN model on thermoelastic interaction in an infinite fibre- reinforced anisotropic plate containing a circular hole", *J. Comput. Theor. Nanosci.*, **11**(2), 380-384. https://doi.org/10.1166/jctn.2014.3363.

Abbas, I.A. (2015), "Eigenvalue approach on fractional order theory of thermoelastic diffusion problem for an infinite elastic medium with a spherical cavity", *Appl. Math. Model.*, **39**(20), 6196-6206. https://doi.org/10.1016/j.apm.2015.01.065.

Abo-Dahab, S. and Lotfy, Kh. (2015), "Generalized magneto-thermoelasticity with fractional derivative heat transfer for a rotation of a fibre-reinforced thermoelastic", *J. Comput. Theor. Nanosci.*, **12**(8), 1869-1881. https://doi.org/10.1166/jctn.2015.3972.

Aboelregal, A.E., Ahmed, I.E., Nasr, M.E., Khalil, M., Zakria, A., and Mohammed, F.A. (2020), "Thermoelastic processes by a continuous heat source line in an infinite solid via Moore-Gibson-Thompson thermoelasticity", *Mater. (Basel)*, **13**(19), 4463. https://doi.org/10.3390/ma13194463.

Abouelregal, A., Elagan S.K. and Alshehri, N. (2021), "Modified Moore-Gibson-Thompson photo thermoelastic model for a rotating semiconductor half-space subjected to a magnetic field", *Int. J. Modern Phys.*, **32**(12), 2150163. https://doi.org/10.1142/s0129183121501631.

Abouelregal, A., Ersoy, H. and Civalek, Ö. (2021), "Solution of Moore-Gibson-Thompson equation of an unbounded medium with a cylindrical hole", *Math.*, **9**(13), 1536. https://doi.org/10.3390/math9131536.

Almond, D.P. and Patel, P.M. (1996), *Photothermal Science and Techniques*, Chapman and Hall, London.

Bazarra, N., Fernández, J.R. and Quintanilla, R. (2020), "Analysis of a Moore-Gibson-Thompson thermoelastic problem", *J. Comput. Appl. Math.*, **382**, 113058. https://doi.org/10.1016/j.cam.2020.113058.

Biot, M.A. (1956), "Thermoelasticity and irreversible thermodynamics", *J. Appl Phys.*, **27**(3), 240-253. https://doi.org/10.1063/1.1722351.

Conti, M., Pata, V. and Quintanilla, R. (2020a), "Thermoelasticity of Moore-Gibson-Thompson type with history dependence in the temperature", *Asymp. Anal.*, **120**, 1-21. https://doi.org/10.3233/ASY-191576.

Conti, M., Pata, V. and Quintanilla, R. (2020b), "On the analyticity of the MGT- viscoelastic plate with heat conduction", *J. Diff. Equ.*, **269**(10), 7862-7880. https://doi.org/10.1016/j.jde.2020.05.043.

Dhaliwal, R.S. and Singh, A. (1983), "Dynamic coupled thermoelasticity", *SIAM Rev.*, **25**(1), 126-127.

Green, A.E. and Naghdi, P.M. (1991), "A re-examination of the basic postulates of thermomechanics", *Proc. Roy. Soc. London A,* **432**, 171-194. https://doi.org/10.1098/rspa.1991.0012.

Green, A.E. and Naghdi, P.M. (1992), "On undamped heat waves in an elastic solid", *J. Therm. Stress.,* **15**, 253-264. https://doi.org/10.1080/01495739208946136.

Green, A.E. and Naghdi, P.M. (1993), "Thermoelasticity without energy dissipation", *J. Elast.*, .**31**, 189-208. https://doi.org/10.1007/BF00044969.

Hobiny, A. and Abbas, I.A. (2018), "Theoretical analysis of thermal damages in skin tissue induced by intense moving heat source", *Int. J. Heat Mass Transf.*, **124**, 1011-1014. https://doi.org/10.1016/j.ijheatmasstransfer.2018.04.018.

Hobiny, A., Alzahrani, S. and Abbas, A. (2021), "A study on photo-thermo-elastic wave in a semi-conductor

material caused by ramp-type heating", *Alex. Eng. J.*, **60**(2), 2033-2040. https://doi.org/10.1016/j.aej.2020.12.002.

Jahangir, A., Tanvir, F. and Zenkour, A.M. (2020), "Reflection of photothermoelastic waves in a semiconductor material with different relaxations", *Ind. J. Phys.*, **95**, 51-59. https://doi.org/10.1007/s12648-020-01690-x.

Jangid, K., Gupta, M. and Mukhopadhyay, S. (2021), "On propagation of harmonic plane waves under the Moore-Gibson-Thompson thermoelasticity theory", *Wave. Random Complex Media*, 1-24. https://doi.org/10.1080/17455030.2021.1949071.

Khamis, A.K., El-Bary, A.A., Lotfy, Kh. and Bakali, A. (2020), "Photothermal excitation processes with refined multi dual phase-lags theory for semiconductor elastic medium", *Alex. Eng. J.*, **59**(1), 1-9. https://doi.org/10.1016/j.aej.2019.11.016.

Kumar, H. and Mukhopadhyay, S. (2020), "Thermoelastic damping analysis in microbeam resonators based on Moore-Gibson-Thompson generalized thermoelasticity theory", *Acta Mech.*, **231**, 3003-3015. https://doi.org/10.1007/s00707-020-02688-6.

Kumar, R., Sharma, N. and Chopra, S. (2022), "Modelling of thermomechanical response in anisotropic photothermoelastic plate", *Int. J. Mech. Eng.*, **7**(6), 577-594.

Lord, H.W. and Shulman, Y. (1967), "A generalized dynamical theory of thermoelasticity", *J. Mech. Phys. Solid.*, **15**(5), 299-309. https://doi.org/10.1016/0022-5096(67)90024-5.

Lotfy, Kh. (2019), "Effect of variable thermal conductivity during the photothermal diffusion process of semiconductor medium", *Silicon,* **11**(4), 1863-1873. https://doi.org/10.1007/s12633-018-0005-z.

Lotfy, Kh. and Othman, M. (2011), "Effect of rotation on plane waves in generalized thermo-microstretch elastic solid with one relaxation time", *Multidisc. Model. Mater. Struct.*, **7**(1), 43- 62. https://doi.org/10.1108/15736101111141430.

Lotfy, Kh., Hassan, W., El-Bary, A.A. and Kadry, M.A. (2020), "Response of electromagnetic and Thomson effect of semiconductor medium due to laser pulses and thermal memories during photothermal excitation", *Result. Phys.*, **16**, 102877. https://doi.org/10.1016/j.rinp.2019.102877.

Mahdy, A.M.S., Lotfy, Kh., Ahmed, M.H., El-Bary, A.A. and Ismail, E.A. (2020), "Electromagnetic hall current effect and fractional heat order for microtemperature photo-excited semiconductor medium with laser pulses", *Result. Phys.*, **17**, 103161. https://doi.org/10.1016/j.rinp.2020.103161.

Mandelis, A. (1987), *Photoacoustic and Thermal wave Phenomena in Semiconductors*, Elsevier Science, North- Holland, New York.

Mandelis, A. and Michaelian, K.H. (1997), "Photoacoustic and photothermal science and engineering" *Opt. Eng.*, **36**(2), 301-302. https://doi.org/10.1117/1.601597.

Marin, M., Öchsner, A. and Bhatti, M.M. (2020), "Some results in Moore-Gibson-Thompson thermoelasticity of dipolar bodies", *ZAMM-J. Appl. Math. Mech.*, **100**(2), e202000090. https://doi.org/10.1002/zamm.202000090.

Marin, M., Othman, M. and Abbas, I.A. (2015), "An extension of the domain of influence theorem for generalized thermoelasticity of anisotropic material with voids", *J. Comput. Theor. Nanosci.*, **12**(8), 1594-1598. https://doi.org/10.1166/jctn.2015.3934.

Mohamed, M.S., Lotfy, Kh., El-Bary, A. and Mahdy, A.M.S. (2022), "Photo-thermal-elastic waves of excitation microstretch semiconductor medium under the impact of rotation and initial stress", *Opt. Quant. Electron.*, **54**(4), 1-21. https://doi.org/10.1007/s11082-022-03533-x.

Nikolic, P.M. and Todorovic, D.M. (1989), "Photoacoustic and electroacoustic properties of semiconductors", *Prog. Quant. Electron.*, **13**, 107-189.

Othman, M., Lotfy, Kh. and Farouk, R. (2009), "Transient disturbance in a half-space under generalized magneto-thermoelasticity with internal heat source", *Acta Physica Polonica A*, **116**(2), 185-192.

Quintanilla, R. (2019), "Moore-Gibson-Thompson thermoelasticity", *Math. Mech. Solid.*, **24**(12), 4020-4031. https://doi.org/10.1177/ 1081286519862007.

Quintanilla, R. (2020), "Moore-Gibson-Thompson thermoelasticity with two temperatures", *Appl. Eng. Sci.*, **1**, 100006. https://doi.org/10.1016/j.apples.2020.100006.

Roychoudhari, S.K. (2007), "On a thermoelastic three-phase-lag model", *J. Therm. Stress.*, **30**, 231-238.

https://doi.org/10.1080/01495730601130919.

Saeed, A.M., Lotfy, Kh., El-Bary, A. and Ahmed, M.H. (2022), "Functionally graded (FG) magneto-photo-thermoelastic semiconductor material with hyperbolic two-temperature theory", *J. Appl. Phys.*, **131**(4), 045101. https://doi.org/10.1063/5.0072237.

Sharma, K. (2010), "Boundary value problems in generalised thermodiffusive elastic medium", *J. Solid. Mech.*, **2**(4), 348-362.

Sharma, N. and Kumar, R. (2021), "Photo-thermoelastic investigation of semiconductor material due to distributed loads", *J. Solid Mech.*, **13**(2), 202-212. https://doi.org/10.22034/JSM.2020.1907462.1639.

Sharma, N. and Kumar, R. (2022), "Photothermoelastic deformation in dual phase lag model due to concentrated inclined load", *Itali. J. Pure Appl. Math.*.

Sharma, S., Sharma, K. and Bhargava, R.R. (2013), "Propagation of waves in micropolar thermoelastic solid with two temperatures bounded with layers or half-space of inviscid liquid", *Mater. Phys. Mech.*, **16**, 66-81.

Singh, B. and Mukhopadhyay, S. (2021), "Galerkin-type solution for the Moore-Gibson-Thompson thermoelasticity theory", *Acta Mechanica*, **232**, 1273-1283. https://doi.org/10.1007/s00707-020-02915-0.

Thompson, P.A. (1972), *Compressible-Fluid Dynamics*, New York: McGraw-Hill.

Tzou, D.Y. (1995), "A unified approach for heat conduction from macro-to-micro-scales", *J. Heat Transf.*, **117**(1), 8-16. https://doi.org/10.1115/1.2822329.

Zakaria, K., Sirwah, M.A. and Abouelregal, A.E. (2021), "Photo-thermoelastic model with time- fractional of higher order and phase lags for a semiconductor rotating materials", *Silicon*, **13**, 573-585. https://doi.org/10.1007/s12633-020-00451-z.

Zenkour, A.M. (2020), "Exact coupled solution for photothermal semiconducting beams using a refined multi-phase-lag theory", *Opt. Laser Technol.*, **128**, 106233. https://doi.org/10.1016/j.optlastec.2020.106233.

DC